RSC Advances

PAPER

View Article Online
View Journal | View Issue

Cite this: *RSC Adv.*, 2021, **11**, 26876

3D hollow-structured hydrogels with editable macrostructure, function, and mechanical properties induced by segmented adjustments†

Qinhua Wang,‡[a] Jing Yu,‡[a] Xingmei Lu,[a] Shilin Cao,[a] Lihui Chen,[a] Xiaofeng Pan,*[b] Yonghao Ni*[ac] and Xiaojuan Ma *[a]

Currently, it is challenging to prepare uniform hollow-structured hydrogels with tailorable comprehensive properties. Herein, making full use of the different gelation routes of polyvinyl alcohol (PVA), we propose a distinctive two-stage method for preparing hollow-structured hydrogels, which is to arrange the microstructure of the hydrogel through segmented adjustment. The mechanical properties, macrostructure, and functions of the obtained hollow hydrogel can be easily designed and edited. Specifically, the mechanical properties of the hollow hydrogel can be improved from "soft" to "hard" by changing the preparation conditions. In addition, hollow hydrogels with diverse macrostructures can also be developed through different templates, such as tubes, gloves, and rings. More importantly, the hollow hydrogels can be endowed with conductive, anti-drying, anti-freezing, and photothermal-converting functions due to the great system compatibility of the gel precursor. Benefiting from the advantages of the hollow hydrogel, the conductive gel ring-based bioelectrodes and sensors were developed. Interestingly, the adaptive gel ring-based electronics can stably record the electrophysiological and strain signals of the human body without the help of adhesive tape. This study opens more opportunities for development and applications of other hydrogel-based hollow materials.

Received 11th July 2021
Accepted 26th July 2021

DOI: 10.1039/d1ra05338h

rsc.li/rsc-advances

1. Introduction

3D hollow-structured hydrogels have gradually received widespread attention from biology, chemistry, to the latest flexible electronics and interdisciplinary fields.[1–3] In view of the high-water content, adjustable strength and elasticity, tissue compatibility, and designable functionality of the hydrogels, 3D hollow hydrogels can be applied in tissue/cell scaffolds, microfluidic chips, and drug delivery carriers, as well as wearable electronics.[4–8]

The most commonly used preparation method for the hollow structure of hydrogels is to convert the liquid precursor to a solid hollow hydrogel. For example, the *in situ* polymerization of monomers is catalyzed by modifying the template surface to produce hollow hydrogel components/coatings.[9,10] However, it is difficult to maintain the uniformity of the cross-link density distribution in the radial direction of the hollow hydrogel due to the limitation of the surface reaction. Similarly, the thickened gel precursor can be coated on the surface of the template and then assembled into a hollow hydrogel/coating.[11] Unfortunately, the higher fluidity of the thickening liquid greatly limits the construction of a uniform and thick hollow gel structure.[12] In addition, the liquid–solid conversion method on the template surface also needs to overcome the strong affinity of the gel and the template, which causes the final product to be difficult to peel off.[12,13] Currently, the precise construction of a uniform hollow hydrogel can be assisted by 3D printing technology.[14] The rigid requirements of advanced equipment, complex printing procedures, and precise raw material ratios are often disadvantageous for the simple and large-scale preparation of hollow hydrogels.[15]

Moreover, the evolution from solid gel to hollow gel is also regarded as an effective method to prepare the hollow structure of hydrogel.[16] The Cui group proposed to immerse the dynamic hydrogel in an ionic solution to de-crosslink and migrate part of the polymer, thereby realizing the construction of hollow tubes and spheres of hydrogel.[17] The cavitation of the hydrogel induced by the adjustment of microstructures brings a broader idea to the casting of hollow hydrogels. Nevertheless, there are still many uncontrollable factors in the above-mentioned

[a]*College of Material Engineering, Fujian Agriculture and Forestry University, Fuzhou City, Fujian Province 350002, People's Republic of China. E-mail: 1212juanjuan@163.com*

[b]*Centre for Energy, Materials and Telecommunications, Institut National de la Recherche Scientifique, 1650 Boulevard Lionel-Boulet, Varennes, Québec J3X 1S2, Canada. E-mail: xiaofeng.pan@inrs.ca*

[c]*Limerick Pulp and Paper Centre, Department of Chemical Engineering, University of New Brunswick, Fredericton, New Brunswick E3B5A3, Canada. E-mail: yonghao@unb.ca*

† Electronic supplementary information (ESI) available. See DOI: 10.1039/d1ra05338h

‡ Q. W. and J. Y. contributed equally to this work.

immersion/reaction process. The size of the gel cavity is not easy to adjust, and the construction of additional functions to the cavity gel will also be hindered.[18] The plasticine can usually be molded into different shapes at will. If there is a plasticine-like hydrogel, coating it on the surface of the template will lead to the construction of hollow hydrogels. For example, the PVA–glycerol–borax hydrogel we previously reported can deform and stretch at will like plasticine.[19] However, this is far inferior to the mechanical properties of the PVA hydrogel prepared by the traditional freeze–thaw process or the binary solvent system. Therefore, this type of hydrogels may inherit the weak strength of the plasticine-like gel and cannot meet the subsequent use requirements.[19–22]

Herein, the segmental adjustment of the microstructure of the hydrogel by the combination of plasticizer and freeze–thaw means enables the PVA–borax hydrogel to achieve plasticine-like plasticity and rubber-like strength successively. This method cleverly combines the softening effect of glycerin on the PVA–borax hydrogel and the enhancement effect of the freeze–thaw treatment on the PVA–glycerin–borax gel. This allows the hydrogel to achieve initial deformation and subsequent permanent solidification. With the help of templates, we carefully realized the preparation of editable hollow hydrogel components for the first time. The resultant hollow hydrogel not only has adjustable mechanical properties and macrostructures, but also has great degradability. In addition, the wide compatibility of the gel precursor is conducive to the hollow gel to achieve designable functionality, such as electrical conductivity, anti-freeze, anti-dryness, and photothermal conversion. Importantly, the conductive hydrogel ring was used for the first time as an adhesive-free and self-adaptable bioelectrode and sensor for collecting physiological and motion signals of the human body. This research not only provides a feasible route for the construction of designable hollow gel, but also proves the huge advantages of hollow gels in wearable electronics.

2. Results and discussion

Fig. 1 exhibits in detail the design and preparation process of the gel hollow structure. First, a borax cross-linked PVA hydrogel was prepared (Fig. 1a), which has soft and easily fractured

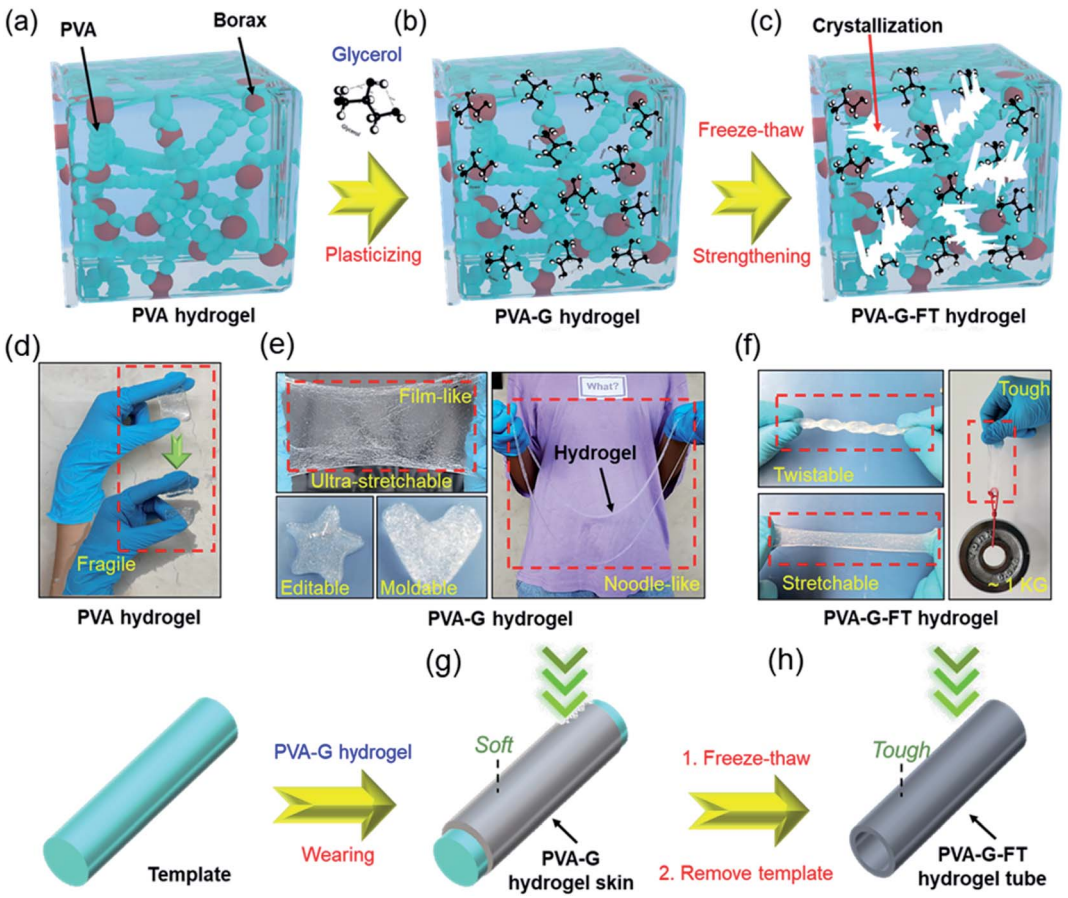

Fig. 1 (a–c) The segmental adjustment of the hydrogel microstructure by the combination of plasticizer and freeze–thaw means enables the PVA–borax hydrogel to achieve plasticine-like plasticity and rubber-like strength successively. (d) PVA hydrogel is easily broken after slight stretching. (e) PVA–G hydrogel has great stretchability, editability, and mouldability. (f) PVA–G-FT hydrogel has great toughness and strength. (g) The plasticine-like PVA–G hydrogel is used as skin for coating on the surface of a template. (h) The hollow PVA–G-FT hydrogel with template removed.

mechanical properties (Fig. 1d). In order to improve the stretchability and plasticity of the hydrogel, the plasticizer glycerol was incorporated into the hydrogel system to obtain a plasticine-like PVA–glycerol (PVA–G) hydrogel (Fig. 1b). The addition of glycerol obviously enhances the stretchability and re-moldability of the hydrogel. This is because glycerol can improve the fluidity of the PVA chains.[23–25] In addition, the strong hydrogen bond between glycerol and PVA also hinders the formation of intra- and inter-chain hydrogen bonds of PVA, thereby affecting the crosslinking and alignment of the polymer.[25] As presented in Fig. 1e, PVA–G hydrogel can be stretched and molded into film, a five-pointed star, heart, and even noodle-like long strips. Consistent with the above assumption, the plasticine-like PVA–G hydrogel can be easily coated on the solid template without flowing randomly (Fig. 1g). The low adhesion of PVA–G hydrogel also reduces the difficulty of peeling the gel from the template. Therefore, the construction of PVA–G hydrogel is beneficial to the rapid construction of the hollow structure of the gel. Unfortunately, the plasticine-like mechanical properties of PVA–G hydrogel also makes it difficult for hollow structure to maintain stability. Here, we innovatively applied another hydrogel forming method of PVA to

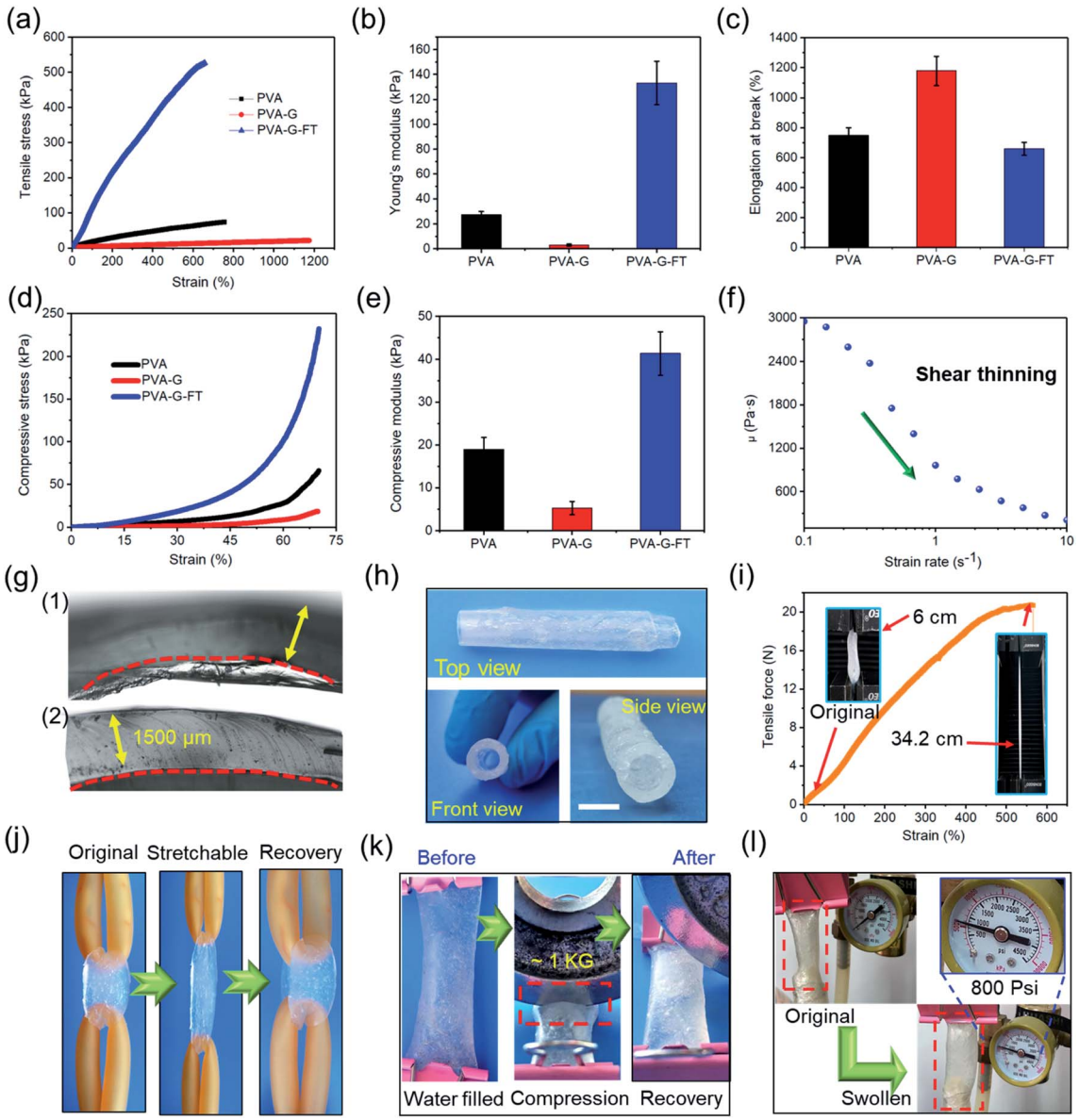

Fig. 2 (a) Typical tensile stress–strain curve, (b) Young's modulus, and (c) elongation at break for PVA, PVA–G, and PVA–G-FT hydrogels. (d) Typical compressive stress–strain curve and (e) compressive modulus for PVA, PVA–G, and PVA–G-FT hydrogels. (f) Variation of viscosity in variable frequency scanning of PVA–G hydrogel (typical shear thinning properties). (g) Optical micrograph of the interface of the hollow (1) PVA–G and (2) PVA–G-FT hydrogel tubes (with template). (h) Three-view drawing of PVA–G-FT hydrogel tube. Scale bar: 5 mm (i) tensile force–strain curve for PVA–G-FT hydrogel tube. (j and k) Elasticity, recoverability, anti-compression of PVA–G-FT hydrogel tube. (l) Photographs showing low elastic expansion of the PVA–G-FT hydrogel tube under 800 psi nitrogen flow. Note that all hydrogel tubes used for testing have a same thickness of 1.5 mm and a same inner diameter of 5 mm.

reinforce the hollow structure. Specifically, the template coated with the PVA–G hydrogel was subjected to freezing–thawing (FT) processing to strengthen the PVA–G gel to obtain the PVA–G-FT hydrogel (Fig. 1c, f, and h). The principle of reinforcement is that the soft PVA–G gel can be treated with FT to form a strong physical crystalline area to increase its strength (Fig. S1†).[20,26] Moreover, PVA–G-FT hydrogel has good degradability (Fig. S2†).

The mechanical properties of the hydrogel at different stages are further determined. As depicted in Fig. 2a–e, glycerol greatly improves the stretchability of the hydrogel, while also reducing the hydrogel strength (including compressive and tensile modulus). Therefore, the extremely soft PVA–G hydrogel (Young's modulus: ~3 kPa) is very easy to deform and has great re-moldability. At the same time, the super stretchability (~1170%) of PVA–G hydrogel can help prevent the gel from easily breaking during the expansion process. The change in viscosity of PVA–G hydrogel with frequency also further proves that it has good shear thinning properties (Fig. 2f).[27]

The FT process significantly improves the strength of the hydrogel (Young's modulus: ~133 kPa), with only a small decrease in the stretchability (~650%) of the gel. Therefore, the strong PVA–G-FT hydrogel can realize the construction of stable hollow structure. More importantly, the mechanical properties of the final hydrogel can be adjusted by changing the PVA contents (Fig. S3†) and freezing time (Fig. S4†) to meet the needs of the hollow structure under specific conditions. Benefiting from tailoring the two-stage gel microstructure, the hydrogel can be constructed to the appropriate hollow structures.

Here, a strong hollow hydrogel tube was assembled using the above method, and together with detailed mechanical properties, was characterized. As exhibited in Fig. 2g, the PVA–G-FT hydrogel tube is obviously more compact and has a flatter section, which proves that it has a more stable structure. Fig. 2h exhibits the free-standing and hollow tubular structure after removing the template. In Fig. 2i, the maximum elongation (strain) of the gel tube is ~600%, and the maximum strain load of ~20 N can be generated. The gel tube retracted to its original shape after being stretched violently, which also proved its good resilience (Fig. 2j). The water tightness of the gel tube proved to be excellent. In Fig. 2k, the gel tube filled with water was sealed and then rolled with a 1 kg disc, without cracking or water leakage. Therefore, the hydrogel tube has the potential as a liquid transport tube in biological tissue engineering. In addition, the compact structure of the gel also promotes its great gas tightness, which can withstand at least 800 psi of air

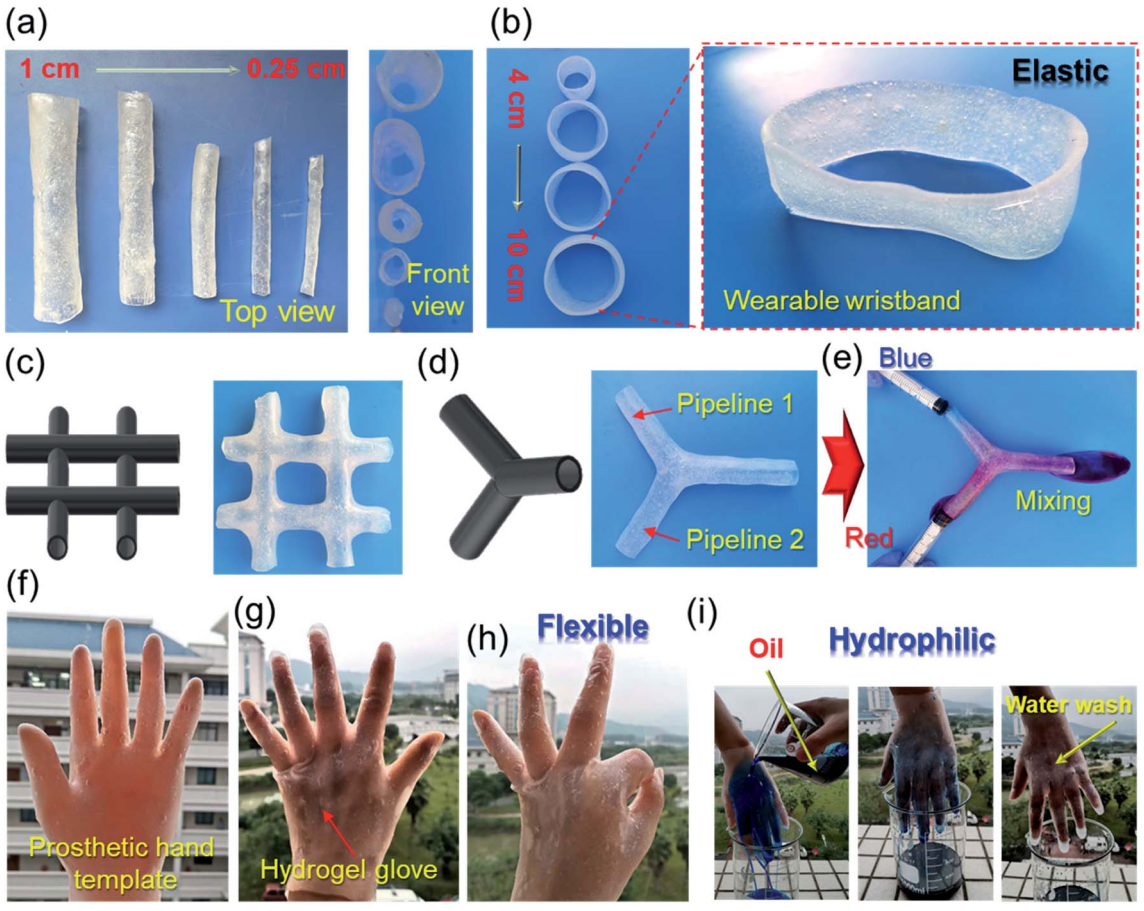

Fig. 3 (a) Hydrogel tubes and (b) hydrogel rings with different inner diameters. The (c) #-type and (d) three-way hydrogel molds and hollow hydrogel tubes. (e) The actual application picture of the gel-based two-liquid mixing pipes. (f) Picture of the prosthetic hand template with hydrogel skin. (g and h) Picture of the human hand with flexible hydrogel glove. (i) Picture of the hydrophilic hydrogel glove.

pressure (Fig. 2l), so it can be used for gas transportation in the human body or medical equipment. In short, the elasticity, stretchability, strength, air tightness, and water tightness of the gel tube assembled by the two-stage method are very good.

On the other hand, due to the great ductility and self-healing of PVA–G gel, hollow tubes with inner diameters ranging from 0.25 cm to 1 cm can be developed by combining templates of different shapes (Fig. 3a). Of course, larger size gel rings (d: 4–10 cm) can also be fabricated (Fig. 3b). Interestingly, with different molds, complex hollow structures can also be easily manufactured. Fig. 3c and d presents the #-tape and the three-way hollow tube assembled by the hydrogel. Among them, Fig. 3e also records the actual application picture of the gel-based two-liquid mixing pipes. In addition, we have also developed a complex hydrogel-based glove (Fig. 3f–g) using prosthetic hand mold, which has proven to be very flexible and hydrophilic (Fig. 3h–i).[28] In fact, the gel skin on the surface of the template can not only be peeled off to prepare a hollow tube, the gel skin can also not be peeled off to improve the hydrophilicity, surface flexibility, biocompatibility and other functionalities of the template substrate.[29] This is another interesting application.

In addition to adjustable strength and macrostructure, the hollow gel also has great system compatibility, so that the hollow gel tube can be given designable functionality by adding nano additives or post-treatment. For example, the prepared hydrogel tube is soaked in glycerol for solvent replacement, and finally a gel tube with anti-drying and anti-freezing properties is obtained (Fig. 4a–d). At the same time, glycerol soaking can further improve its strength (Fig. S5†). This is beneficial to increase its service life and expand its applications. Similarly, hydrophilic CNTs are incorporated into the gel precursor, and finally a conductive composite tube can be assembled (Fig. 4e and f). In addition, after proanthocyanins (PC) are incorporated, a composite tube with photothermal effect can be finally obtained, which responds well to near-infrared light and gradually convert it into heat (Fig. 4g and h).[30] This process was fully recorded by the near-infrared camera (Fig. 4i).

So far, it has been proven that the functionality, macrostructure, and mechanical properties can be pre-designed/adjusted. Based on the advantages of the hydrogel tube, we first developed a series of wearable electronic devices of the hydrogel hollow structure. First, a hydrophilic CNT-doped conductive hydrogel ring is manufactured, which inherits the excellent tensile resilience of the gel ring and the excellent conductivity of CNT (Fig. 5a and 4f). Next, the conductive gel ring is used to monitor electrophysiological signals in the human body, recording the movement discharge phenomenon

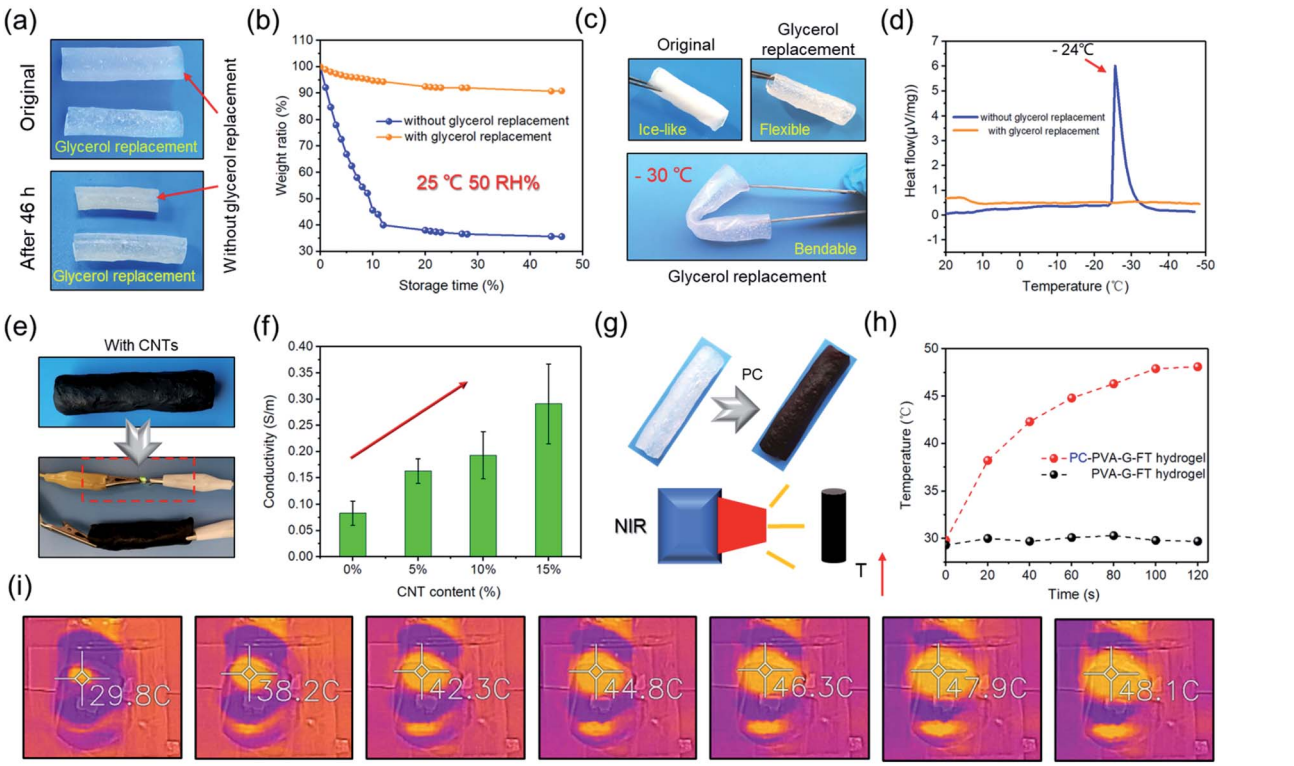

Fig. 4 (a) Photographs of the PVA–G-FT hydrogel tubes with or without glycerol replacement after storage for 46 h at 25 °C and 50 RH%. (b) Weight changes of the PVA–G-FT hydrogel tubes with or without glycerol replacement at 25 °C and 50 RH%. (c) Photographs of the PVA–G-FT hydrogel tubes with or without glycerol replacement after storage for 24 h at −30 °C. (d) DSC thermograms of the PVA–G-FT hydrogel with or without glycerol replacement from 20 °C to −48 °C. (e) The conductive PVA–G-FT hydrogel tube containing carbon nanotubes (CNTs) can light up LED lights. (f) The conductivity of hydrogel tube with various CNTs. (g) PVA–G-FT hydrogel tube containing PC with near-infrared photothermal conversion. (h) The temperature of the hydrogel tube with PC or without PC exposed to NIR irradiation (808 nm) for different periods of time. (i) Infrared thermographs of PVA–G-FT hydrogel tube containing PC under NIR irradiation (808 nm).

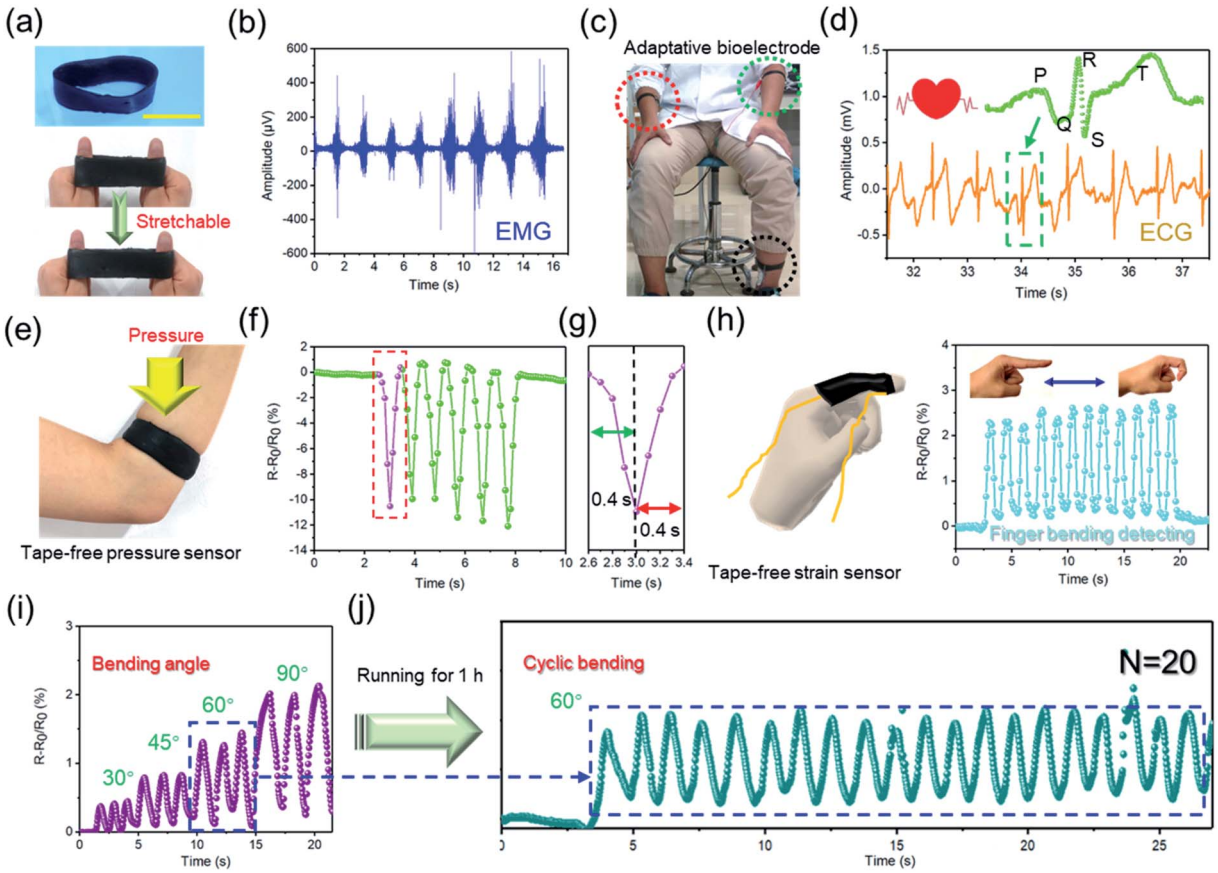

Fig. 5 (a) Schematic illustration of stretchable conductive hydrogel ring. Scale bar: 5 cm. (b) ECG signal collected by hydrogel ring-based bioelectrodes. (c) Schematic illustration of adaptive ring-based bioelectrodes to collect human ECG signals. (d) ECG signal collected by hydrogel ring-based bioelectrodes. (e) Schematic illustration of tape-free conductive hydrogel ring-based pressure sensor. (f and g) Pressure signal recorded by hydrogel ring-based pressure sensor. (h–j) Schematic illustration of tape-free hydrogel ring-based strain sensor to collect various bending signals of finger.

(EMG signal) of the arm skin (Fig. 5b). The results are similar to those from commercial Ag/AgCl electrodes.[31] However, commercial bioelectrodes are disposable, which is due to the dramatic decrease in the adhesion of the electrolyte hydrogel and structural damage after repeated use.[32] Interestingly, this adaptive hydrogel ring-based bioelectrodes can be used for a long time without the trouble of falling off. In addition, the conductive hydrogel ring has also been proven to clearly record the body's ECG signals (Fig. 5c and d). The elastic hydrogel ring-based electronics have improved wearability, stability, and service life.

Inspired by this, the conductive hydrogel ring is further used as a tape-free wearable sensor. As shown in Fig. 5e and f, the gel ring-based sensor can stably and quickly record external pressure stimuli (Fig. 5g). At the same time, similar hydrogel finger cots can also stably monitor the various bending signals of a human finger (Fig. 5h and i). It is important that this gel sensor has great application stability without the help of tape. Of course, it will also not have the inconvenience of peeling and residue like self-adhesive hydrogel sensors.[33,34] Even after the wearer undergoes vigorous exercise, the hydrogel ring can still fit the human skin well and stably collect the strain signals of the human body (Fig. 5j). In short, hydrogel ring-based electronics will have obvious advantages over traditional self-adhesive sensors or fabric sensors, which are manifested in its better fit, stability, and anti-interference.[35]

3. Conclusions

In conclusion, we developed a two-stage method for preparing hollow-structured PVA-based hydrogels. Specifically, the mechanical properties of the hollow gels can be improved from "soft" to "hard". In addition, hollow hydrogels with diverse macrostructures can also be developed through different templates. More importantly, the hollow hydrogel can be endowed with various functions. Benefiting from the advantages of hollow hydrogel, the conductive hydrogel ring can stably record the electrophysiological sand strain signals of the human body without the help of adhesive tape. This study opens more opportunities to the development and applications of other hydrogel-based hollow materials.

Author contributions

The manuscript was written by contributions from all the authors. Q. W. and X. P. conceived the idea, performed the

experiments and wrote the manuscript. J. Y. also carried out some of the experiments. S. C., X. L., L. C., X. M., and Y. N. revised the manuscript.

Conflicts of interest

There are no conflicts to declare.

Acknowledgements

The authors are grateful to the Scientific Research Foundation of Graduate School of Fujian Agriculture and Forestry University (324-1122yb077).

References

1 S. Wu, H. Dong, Q. Li, G. Wang and X. Cao, *Carbohydr. Polym.*, 2017, **168**, 147–152.
2 Y. Yu, H. Yuk, G. A. Parada, Y. Wu, X. Liu, C. S. Nabzdyk, K. Youcef-Toumi, J. Zang and X. Zhao, *Adv. Mater.*, 2019, **31**, 1807101.
3 C. Zhao, P. Zhang, R. Shi, Y. Xu, L. Zhang, R. Fang, T. Zhao, S. Qi, L. Jiang and M. Liu, *Sci. China Mater.*, 2019, **62**, 1332–1340.
4 I. M. El-Sherbiny and M. H. Yacoub, *Glob. Cardiol. Sci. Pract.*, 2017, **2017**(2), 14.
5 S. Ma, M. Rong, P. Lin, M. Bao, J. Xie, X. Wang, W. T. S. Huck, F. Zhou and W. Liu, *Chem. Mater.*, 2018, **30**, 6756–6768.
6 Q. Zhang, X. Liu, X. Ren, F. Jia, L. Duan and G. Gao, *Chem. Mater.*, 2019, **31**, 5881–5889.
7 L. Wu, L. Li, M. Fan, P. Tang, S. Yang, L. Pan, H. Wang and Y. Bin, *Composites, Part A*, 2020, **138**, 106050.
8 J. Yang, X. Zhu, H. Wang, X. Wang, C. Hao, R. Fan, D. Dastan and Z. Shi, *Composites, Part A*, 2020, **131**, 105814.
9 S. Ma, C. Yan, M. Cai, J. Yang, X. Wang, F. Zhou and W. Liu, *Adv. Mater.*, 2018, **30**, 1803371.
10 H. Lin, S. Ma, B. Yu, M. Cai, Z. Zheng, F. Zhou and W. Liu, *Chem. Mater.*, 2019, **31**, 4469–4478.
11 R. Takahashi, K. Shimano, H. Okazaki, T. Kurokawa, T. Nakajima, T. Nonoyama, D. R. King and J. P. Gong, *Adv. Mater. Interfaces*, 2018, **5**, 1801018.
12 Q. Wang, X. Pan, C. Lin, X. Ma, S. Cao and Y. Ni, *Chem. Eng. J.*, 2020, **396**, 125341.
13 L. Han, X. Lu, K. Liu, K. Wang, L. Fang, L.-T. Weng, H. Zhang, Y. Tang, F. Ren, C. Zhao, G. Sun, R. Liang and Z. Li, *ACS Nano*, 2017, **11**, 2561–2574.
14 Q. Liang, F. Gao, Z. Zeng, J. Yang, M. Wu, C. Gao, D. Cheng, H. Pan, W. Liu and C. Ruan, *Adv. Funct. Mater.*, 2020, **30**, 2001485.
15 G. Ying, N. Jiang, C. Parra-Cantu, G. Tang, J. Zhang, H. Wang, S. Chen, N.-P. Huang, J. Xie and Y. S. Zhang, *Adv. Funct. Mater.*, 2020, **30**, 2003740.
16 B. Wu, Y. Jian, X. Le, H. Lin, S. Wei, W. Lu, J. Zhang, A. Zhang, C.-F. Huang and T. Chen, *ACS Appl. Mater. Interfaces*, 2019, **11**, 48564–48573.
17 L. Han, Y. Zheng, H. Luo, J. Feng, R. Engstler, L. Xue, G. Jing, X. Deng, A. del Campo and J. Cui, *Angew. Chem., Int. Ed.*, 2020, **59**, 5611–5615.
18 Y. Tu, Q. Chen, S. Liang, Q. Zhao, X. Zhou, W. Huang, X. Huang and L. Zhang, *ACS Appl. Mater. Interfaces*, 2019, **11**, 18746–18754.
19 X. Pan, Q. Wang, P. He, K. Liu, Y. Ni, L. Chen, X. Ouyang, L. Huang, H. Wang and S. Xu, *Chem. Eng. J.*, 2020, **379**, 122271.
20 X. Pan, Q. Wang, R. Guo, Y. Ni, K. Liu, X. Ouyang, L. Chen, L. Huang, S. Cao and M. Xie, *J. Mater. Chem. A*, 2019, **7**, 4525–4535.
21 F. Chen, D. Zhou, J. Wang, T. Li, X. Zhou, T. Gan, S. Handschuh-Wang and X. Zhou, *Angew. Chem., Int. Ed.*, 2018, **57**, 6568–6571.
22 Q. Rong, W. Lei, L. Chen, Y. Yin, J. Zhou and M. Liu, *Angew. Chem., Int. Ed.*, 2017, **56**, 14159–14163.
23 X. Pan, Q. Wang, P. He, K. Liu, Y. Ni, X. Ouyang, L. Chen, L. Huang, H. Wang and Y. Tan, *ACS Sustainable Chem. Eng.*, 2019, **7**, 7918–7925.
24 X. Pan, Q. Wang, D. Ning, L. Dai, K. Liu, Y. Ni, L. Chen and L. Huang, *ACS Biomater. Sci. Eng.*, 2018, **4**, 3397–3404.
25 L. Xu, S. Gao, Q. Guo, C. Wang, Y. Qiao and D. Qiu, *Adv. Mater.*, 2020, 2004579.
26 R. Surudžić, A. Janković, N. Bibić, M. Vukašinović-Sekulić, A. Perić-Grujić, V. Mišković-Stanković, S. J. Park and K. Y. Rhee, *Composites, Part B*, 2016, **85**, 102–112.
27 Y. Chao, Q. Chen and Z. Liu, *Adv. Funct. Mater.*, 2020, **30**, 1902785.
28 L. Dai, B. Wang, X. An, L. Zhang, A. Khan and Y. Ni, *Carbohydr. Polym.*, 2017, **169**, 9–15.
29 H. Yuk, B. Lu and X. Zhao, *Chem. Soc. Rev.*, 2019, **48**, 1642–1667.
30 H. Ma, Q. Zhou, J. Chang and C. Wu, *ACS Nano*, 2019, **13**, 4302–4311.
31 Q. Wang, X. Pan, C. Lin, D. Lin, Y. Ni, L. Chen, L. Huang, S. Cao and X. Ma, *Chem. Eng. J.*, 2019, **370**, 1039–1047.
32 Z. Jia, Y. Zeng, P. Tang, D. Gan, W. Xing, Y. Hou, K. Wang, C. Xie and X. Lu, *Chem. Mater.*, 2019, **31**, 5625–5632.
33 Q. Wang, X. Pan, X. Wang, H. Gao, Y. Chen, L. Chen, Y. Ni, S. Cao and X. Ma, *Composites, Part B*, 2020, **197**, 108187.
34 J. Bai, R. Wang, M. Ju, J. Zhou, L. Zhang and T. Jiao, *Sci. China Mater.*, 2021, **64**, 942–952.
35 Q. Yan, M. Zhou and H. Fu, *Composites, Part B*, 2020, **201**, 108356.